

Supporting Information

Chemical chain termination resolves the timing of ketoreduction in a partially reducing iterative type I polyketide synthase

Hirokazu Kage,^a Elena Riva,^b James S. Parascandolo,^b Martin F. Kreutzer,^a Manuela Tosin*^b and
Markus Nett*^a

[a] Leibniz Institute for Natural Product Research and Infection Biology, Hans-Knöll-Institute, Adolf-Reichwein-Str. 23, D-07745 Jena, Germany.

[b] Department of Chemistry, University of Warwick, Library Road, Coventry CV4 7AC, UK.

Table of Contents

SI2-SI4	Construction of <i>R. solanacearum</i> mutant strains and isolation of compound 2
SI5-SI6	NMR spectra of compound 2
SI7-SI18	Probe feeding studies and intermediate capture
SI19	References

Experimental section

Strains, culture conditions and plasmids. Bacterial strains and plasmids used in the present study are listed in Table S1. The wild-type and the mutant strains of *Ralstonia solanacearum* GMI1000 were grown at 30 °C in BG medium or in modified $\frac{1}{4} \times$ M63 minimal medium supplemented with 0.2% glucose and 0.02% sodium acetate.^{1,2} When required, antibiotics were added to the culture medium at a concentration of 50 µg/mL (apramycin, kanamycin) or 100 µg/mL (ampicillin). *Escherichia coli* strains were routinely grown in Luria broth (LB) medium at 37 °C.

Table S1. Bacterial strains and plasmids used in this study

Strain or plasmid	Relevant properties ^a	Source or reference
Strains		
<i>R. solanacearum</i>		
GMI1000	wild-type micacocidin producer	3
RS31	$\Delta micC$ mutant	this study
RS36	MicC-KR mutant	this study
<i>E. coli</i>		
DH5 α	F- $\Phi 80lacZ\Delta M15 \Delta(lacZYA-argF)$ U169 <i>recA1 endA1</i> <i>hsdR17</i> (r_K^- , m_K^+) <i>phoA supE44</i> λ - <i>thi-1 gyrA96 relA1</i>	Invitrogen
Plasmids		
pIJ773	apramycin resistance cassette; Am ^r	4
pHiK008c1	pET28a carrying 1.2-kb <i>micC</i> fragment; Km ^r	5
pHiK012	pHiK008c1 carrying Am ^r cassette from pIJ773; Am ^r	5
pHiK013a	pHiK008c1 carrying <i>micC</i> -KR ^{Y1991A} fragment; Km ^r	5
pHiK013	pHiK013a carrying Am ^r - <i>sacB</i> cassette; Am ^r	5
pHiK014	pIJ773 carrying <i>sacB</i> gene; Am ^r	this study

^a Abbreviations: Am^r, apramycin resistance; Km^r, kanamycin resistance

General DNA methods. DNA purification, PCR-based site-directed mutagenesis and transformation experiments were carried out as previously described.^{2,5}

Construction of the $\Delta micC$ mutant strain RS31. The vector for the inactivation of *micC* derived from plasmid pHiK008c1, which harbors a 1.2-kb fragment of the targeted gene.⁵ Initially, pHiK008c1 was digested with BsiWI. Subsequently, an apramycin resistance cassette obtained from pIJ773 by digestion with EcoRI and HindIII was blunt-end cloned into the linearized vector. The resulting plasmid pHiK012 was subsequently used for the transformation of *R. solanacearum* GMI1000.

Homologous recombination yielded the double-crossover mutant strain RS31. The $\Delta micC$ mutation was confirmed by sequencing.

Construction of the MicC-KR mutant strain RS36. Site-directed mutagenesis was performed on the *micC* gene fragment in pHiK008c1. The desired mutation for the Y1991A replacement was introduced by PCR using the primers P17 (5'-GGCGTCTGGGGCTCGCGCCTGCAGATCCCGGCCGGCGCCGCGAACGCCTTCCAGGACGCCCTGGTGCGCCTGCGC-3') and P18 (5'-CACGATATCCGGATATAGTTCCTCC-3'). Subsequently, the sample was treated with DpnI to digest the native, non-mutated DNA template. The remaining circular PCR product carrying the mutation (*i.e.*, pHiK013a) was introduced into *E. coli* DH5 α . At the same time, *sacB* was amplified from pUFR80 with primers P20 (5'-CGACTCGAGTATGATATTTTCTGAATTGTG-3') and P21 (5'-CGACTCGAGTATATAGTTCATATGGGATTC-3') and blunt-end ligated into pJET1.2.⁶ Digestion of the resulting plasmid with XbaI and NotI yielded a 1.9-kb fragment, which was cloned into the corresponding sites of pIJ773 to give pHiK014. Finally, the HindIII-NotI fragment of pHiK014, which contained *sacB* and an apramycin resistance gene, was inserted into pHiK013a to give pHiK013. The latter was used for the transformation of *R. solanacearum* GMI1000. The obtained transformants were selected for double-crossover events by adding 10% sucrose to the cultivation medium. The mutation was confirmed in strain RS36 by sequencing.

Metabolic profiling of *R. solanacearum* strains. Three-day-old cultures were exhaustively extracted with ethyl acetate. After evaporation of the organic solvent, the residues were dissolved in methanol. Metabolic profiles were analyzed by HPLC-MS on an Exactive Orbitrap (Thermo Fisher Scientific). The chromatographic system was equipped with a Betasil 100-3 C₁₈ column (150 × 2.1 mm, 3 μ m pore diameter), and separation was performed using a gradient elution of acetonitrile in water plus 0.1% formic acid (5% → 98% acetonitrile within 15 min; flow rate, 0.2 mL min⁻¹).

Isolation and spectroscopic analysis of 4-methoxy-6-pentyl-2H-pyran-2-one (2). For the isolation of **2**, the mutant strain RS36 was cultivated in 6 L of modified $\frac{1}{4} \times$ M63 medium. The fermentation was carried out in 5-L Erlenmeyer flasks on a rotary shaker (120 rpm) at 30 °C for 9 days. At the end of cultivation, the culture broth was extracted three times with equal amounts of ethyl acetate. The

organic layers were pooled and dried under vacuum. After resuspension in methanol, the sample was chromatographed on a Shimadzu UFLC system equipped with a Eclipse-XDB C8 column (250 x 9.4 mm, 5 μ m pore diameter; Macherey & Nagel) using a gradient elution of methanol in water plus 0.1% trifluoroacetic acid (10% \rightarrow 100% methanol within 30 min; flow rate, 2.5 mL min⁻¹). NMR spectra of compound **2** were recorded at 300 K on a Bruker Avance III 500 MHz spectrometer. For this purpose, the sample was dissolved in methanol-*d*₄. The solvent signal was referenced to δ_{H} 3.31 ppm and δ_{C} 49.0 ppm, respectively.

4-methoxy-6-pentyl-2H-pyran-2-one (2). ¹H-NMR (500 MHz, methanol-*d*₄) δ_{H} [ppm] (*J* [Hz]) 0.92 (3 H, t, *J* 7.0, H-5'), 1.35 (2 H, m, H-3'), 1.36 (2 H, m, H-4'), 1.66 (2 H, quint, *J* 7.5, H-2'), 2.49 (2 H, t, *J* 7.5, H-1'), 3.85 (3 H, s, OMe), 5.53 (1 H, d, *J* 2.3, H-3), 6.01 (1 H, d, *J* 2.3, H-5). ¹³C-NMR (125 MHz, methanol-*d*₄) δ_{C} [ppm] 14.2 (C-5'), 23.3 (C-4'), 27.5 (C-2'), 32.2 (C-3'), 34.3 (C-1'), 56.9 (OMe), 88.1 (C-3), 101.3 (C-5), 167.5 (C-2), 167.8 (C-6), 174.0 (C-4).

Figure S1. $^1\text{H-NMR}$ spectrum of 4-methoxy-6-pentyl-2*H*-pyran-2-one (**2**) in methanol- d_4 .

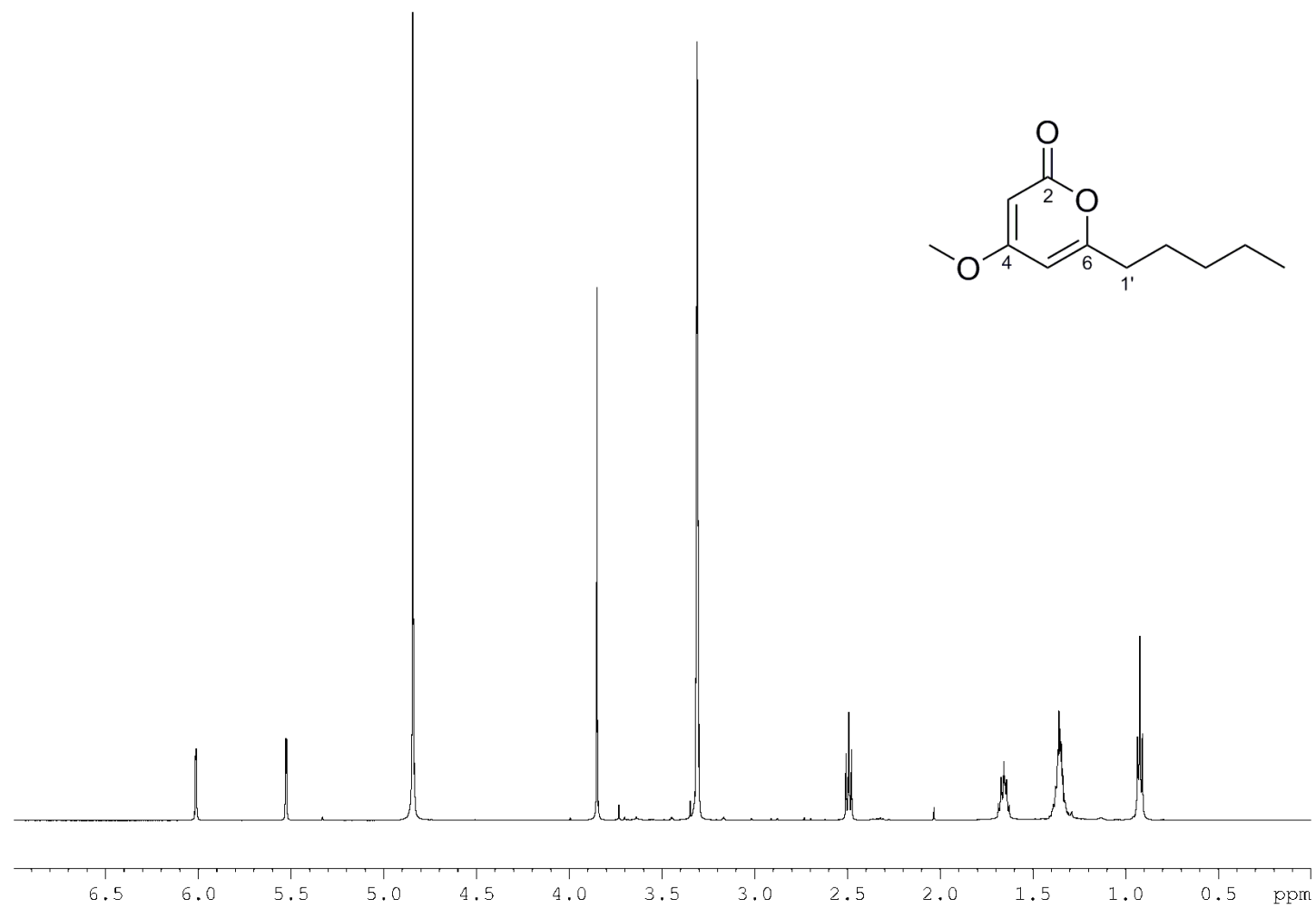
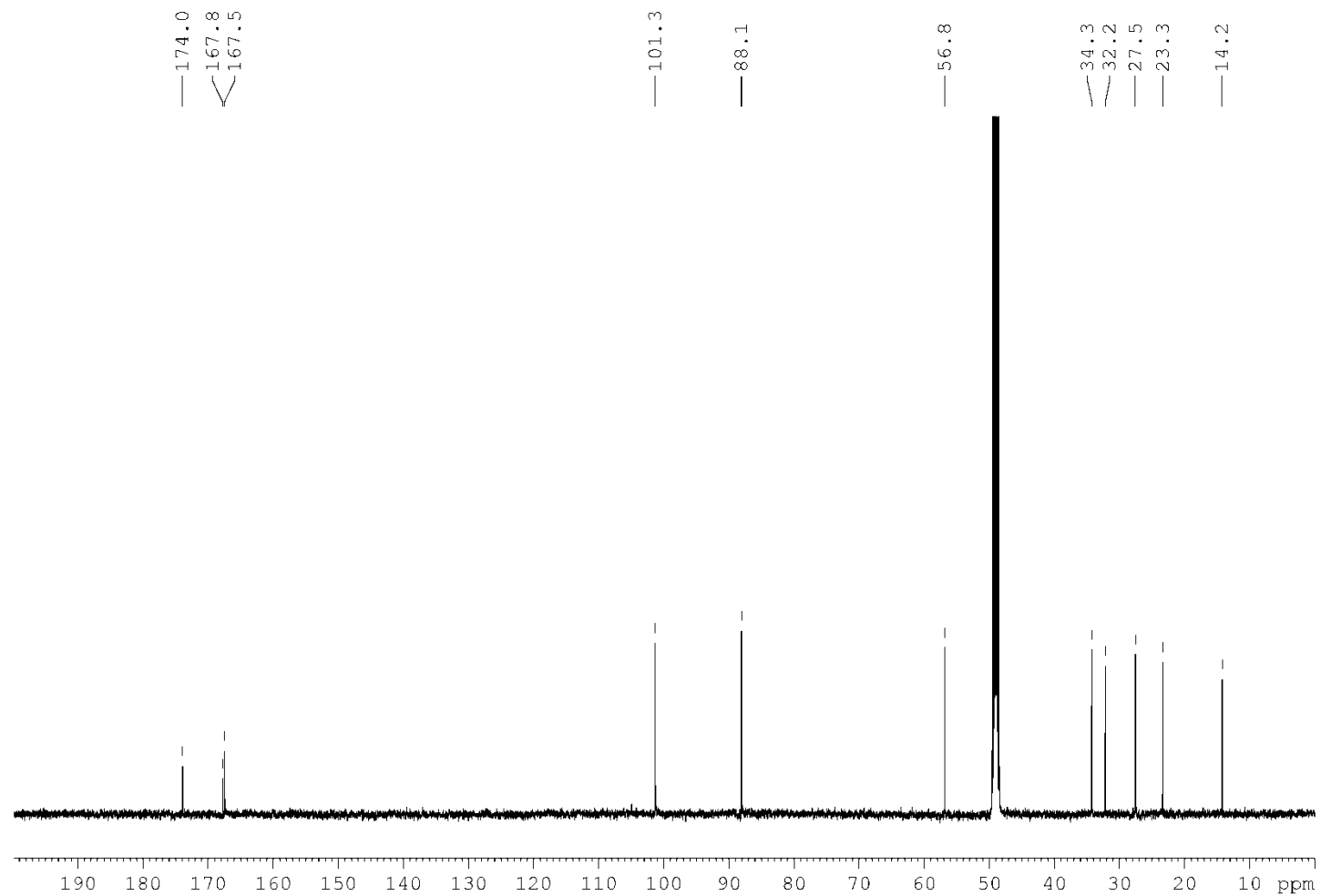


Figure S2. ^{13}C -NMR spectrum of 4-methoxy-6-pentyl-2*H*-pyran-2-one (**2**) in methanol- d_4 .



Cultivation of *R. solanacearum* GMI1000 in the presence of chemical probes. The wild-type strain of *R. solanacearum* GMI1000 was cultured on BG agar at 30 °C for 3 days. The cells of this agar culture were harvested and directly inoculated into modified $\frac{1}{4} \times$ M63 medium. Optical density of the feeding culture was adjusted to a value of 0.2 at a wavelength of 580 nm. For trapping biosynthetic intermediates, chemical chain terminators were added to the feeding culture at the time of inoculation and during the two following days. The daily amount fed was 38.5 μ mol in case of the deuterated and non-deuterated malonyl carba(dethia)-*N*-acetyl cysteamines and 8.3 μ mol in case of methyl 6-decanamide-3-oxohexanoate. On day 4, the cultures were extracted three times with equal amounts of ethyl acetate. The organic layers were pooled and dried under vacuum. The resulting extracts were then redissolved in methanol and subjected to LC-ESI-MS analysis.

Detection and characterisation of biosynthetic intermediates. UPLC-HR-ESI-MS analyses were performed on a MaXis Impact UHR-TOF (Bruker Daltonics). Samples were injected onto an Agilent Eclipse C18 column (100 x 2.1 mm, 1.8 μ m pore diameter). The mobile phase consisted of a gradient of water and acetonitrile (HPLC grade, each with 0.1 % trifluoroacetic acid). The following solvent (A = 1% TFA in H₂O, B = 1% TFA in MeCN) gradients was applied: 5% B 0.0-5.0 min, 5-100% B 5.0-20.0 min; 100% B 20.0-25.0 min; 100-5% B 25.0-27.0; 5% B 27.0-34.0 min. Spectra were recorded in positive ionisation mode, scanning from *m/z* 100 to 3000, with the resolution set at 45K. Selected ion search within 5 ppm was performed for the putative biosynthetic intermediates. Further high resolution analyses for ethyl acetate extracts obtained from *N*-pentynoyl and *N*-decanoyl probes were performed on a Thermo Orbitrap Fusion (Q-OT-qIT, Thermo) instrument. Reversed phase chromatography was used to separate the mixtures prior to MS analysis. Two columns were utilized: an Acclaim PepMap μ -precolumn cartridge (5 x 0.3 mm, 5 μ m pore diameter, 100 Å; Thermo Scientific) and an Acclaim PepMap RSLC (150 x 0.075 mm, 2 μ m pore diameter, 100 Å; Thermo Scientific). The columns were installed on an Ultimate 3000 RSLCnano system (Dionex). Mobile phase buffer A was composed of 0.1% aqueous formic acid and mobile phase B was composed of 100% acetonitrile containing 0.1% formic acid. Samples were loaded onto the μ -precolumn equilibrated in 2% aqueous acetonitrile containing 0.1% trifluoroacetic acid for 8 min at 10 μ L min⁻¹ after which compounds were eluted onto the analytical column. The mobile phase B concentration was set at 50% and maintained for 5

minutes, after which it was increased to 99.5% over 10 min, maintained at 99.5% B over 23 min and then decreased to 50% B over 1 min, followed by a 9 min wash at 50% B. Eluting cations were converted to gas-phase ions by electrospray ionization and analyzed. Survey scans of precursors from m/z 150 to 1500 were performed at 60K resolution (at m/z 200) with a 5×10^5 ion count target. Tandem MS was performed by isolation at 0.7 Th with the quadrupole, HCD fragmentation with normalized collision energy of 30, and rapid scan MS analysis in the ion trap. The MS² ion count target was set to 10^4 and the max injection time was 35 ms. A filter targeted inclusion mass list was used to select the precursor ions. The dynamic exclusion duration was set to 45 s with a 10 ppm tolerance around the selected precursor and its isotopes. Monoisotopic precursor selection was turned on. The instrument was run in top speed mode with 5 s cycles, meaning the instrument would continuously perform MS² events until the list of nonexcluded precursors diminishes to zero or 5 s, whichever is shorter. Fusion runs were performed with Survey scans of precursors from m/z 150 to 1500 at 60K resolution (at m/z 200) with a 1×10^6 ion count target. Tandem MS was performed by isolation at 1.8 Th with the ion-trap, CAD fragmentation with normalized collision energy of 32, and 15K resolution scan MS analysis in the Orbitrap. The data dependent top 20 precursors were selected for MS². MS² ion count target was set to 4×10^6 and the max. injection time was 50 ms. The dynamic exclusion duration was set to 40 s with a 10 ppm tolerance around the selected precursor and its isotopes.

Intermediate capture by probes 3a-b⁷

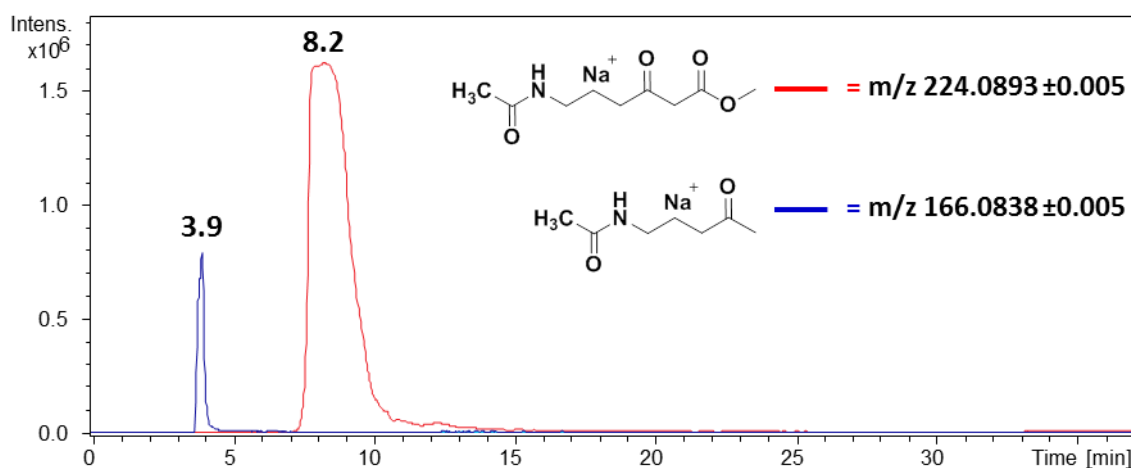


Figure S3. LC-HRMS analyses of the organic extracts of *R. solanacearum* GMI1000 grown in the presence of probe **3a**: $[M+Na]^+$ extracted ion traces for the intact probe (red) and *N*-(4-oxopentyl)acetamide (blue) resulting from *in vivo* hydrolysis and decarboxylation (Bruker MaXis Impact).

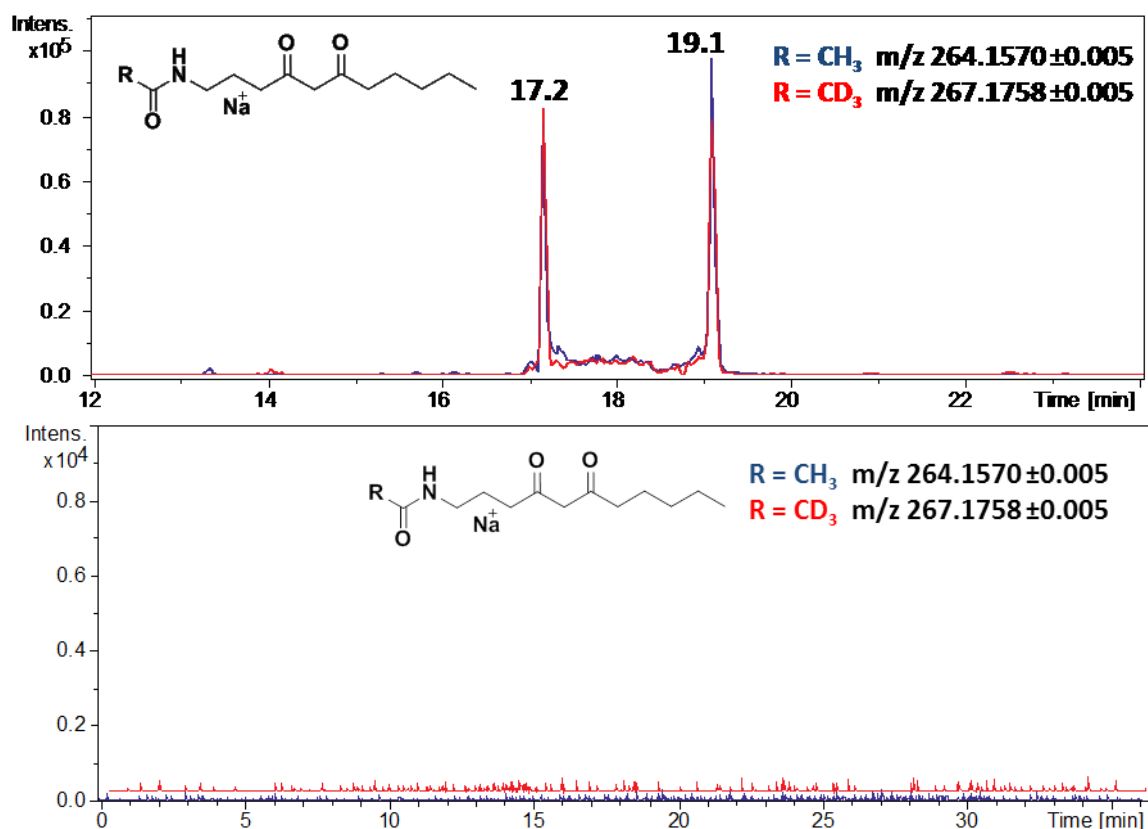


Figure S4. Top: $[M+Na]^+$ extracted ion traces for the putative diketides detected from *R. solanacearum* GMI1000 grown in the presence of probes **3a-b**; bottom: $[M+Na]^+$ extracted ion traces for the same species in a control sample of *R. solanacearum* GMI1000 grown in the absence of **3a-b**. The detection of two peaks for these species is currently under investigation (Bruker MaXis Impact).

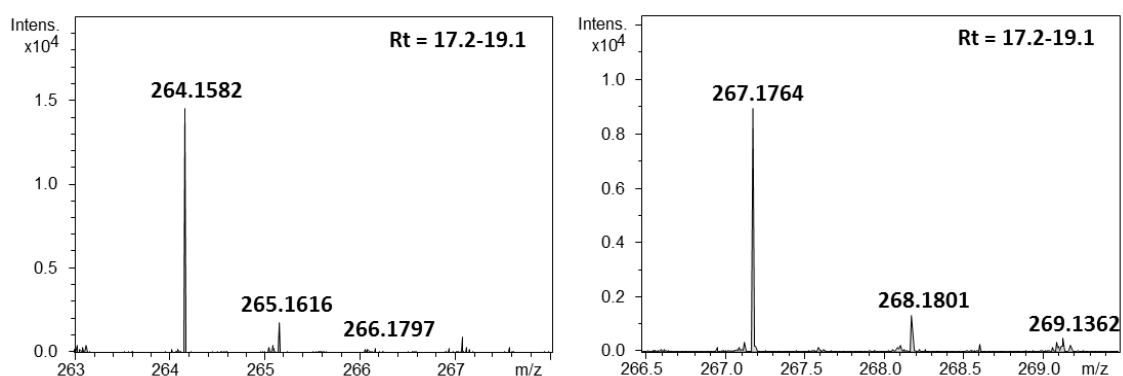


Figure S5. High resolution mass spectra for diketides captured via probe **3a** (left) and **3b** (right) (Bruker MaXis Impact).

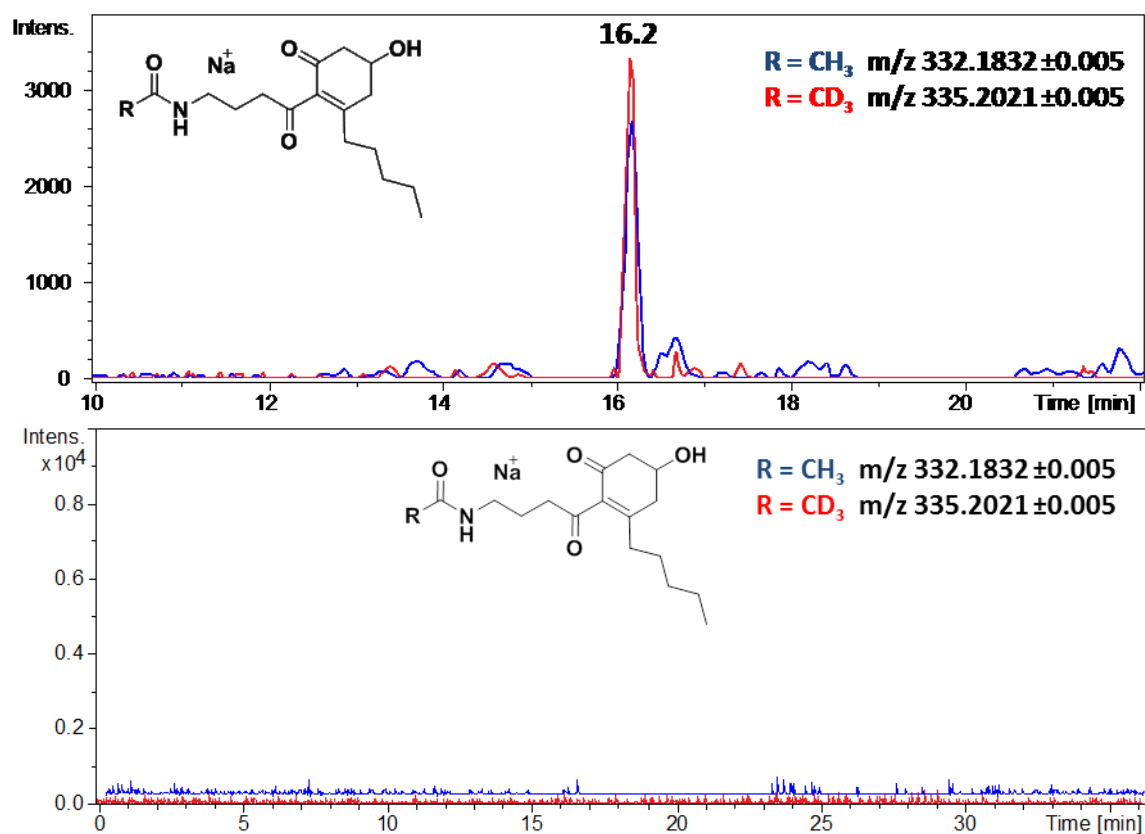


Figure S6. Top: [M+Na]⁺ extracted ion traces for the putative tetraketides detected from *R. solanacearum* GMI1000 grown in the presence of probes **3a-b**; bottom: [M+Na]⁺ extracted ion traces for the same species in a control sample of *R. solanacearum* GMI1000 grown in the absence of **3a-b** (Bruker MaXis Impact).

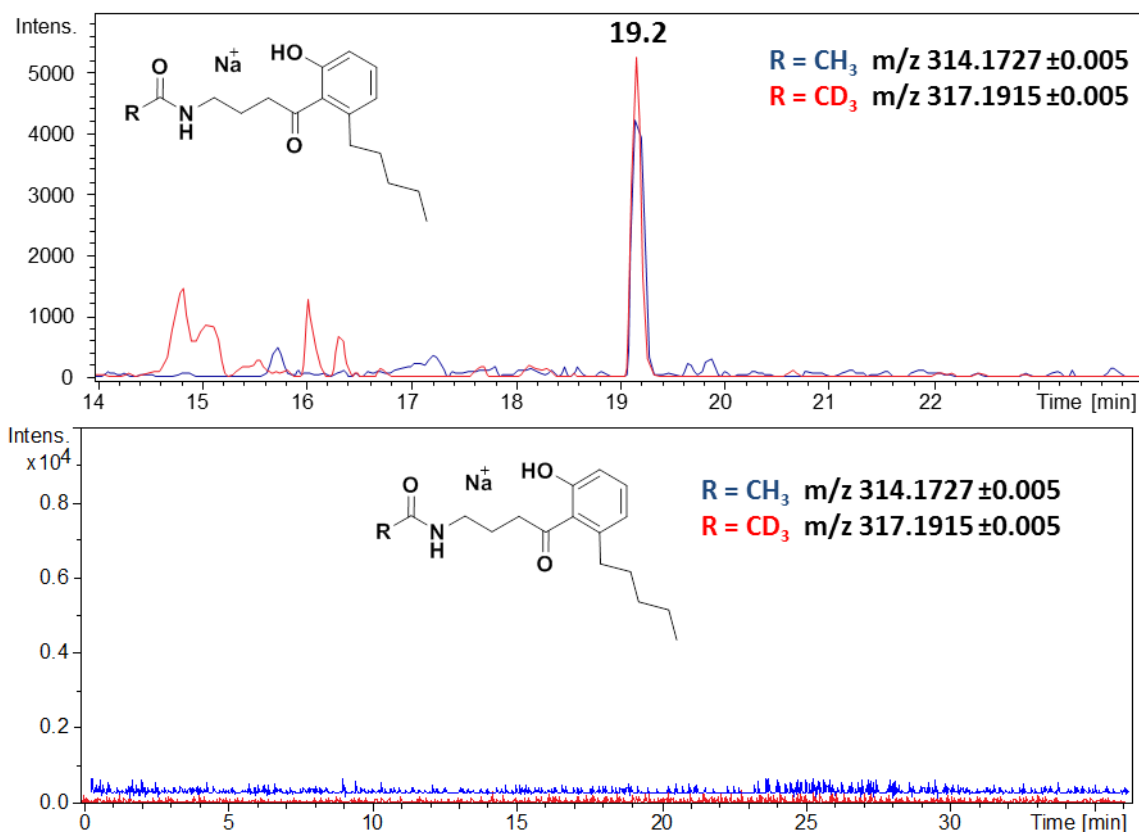


Figure S7. Top: $[\text{M}+\text{Na}]^+$ extracted ion traces for the putative tetraketides detected from *R. solanacearum* GMI1000 grown in the presence of probes **3a-b**; bottom: $[\text{M}+\text{Na}]^+$ extracted ion traces for the same species in a control sample of *R. solanacearum* GMI1000 grown in the absence of **3a-b** (Bruker MaXis Impact).

Intermediate capture by probe 4 (methyl 3-oxo-6-(pent-4-ynamido)hexanoate)⁸

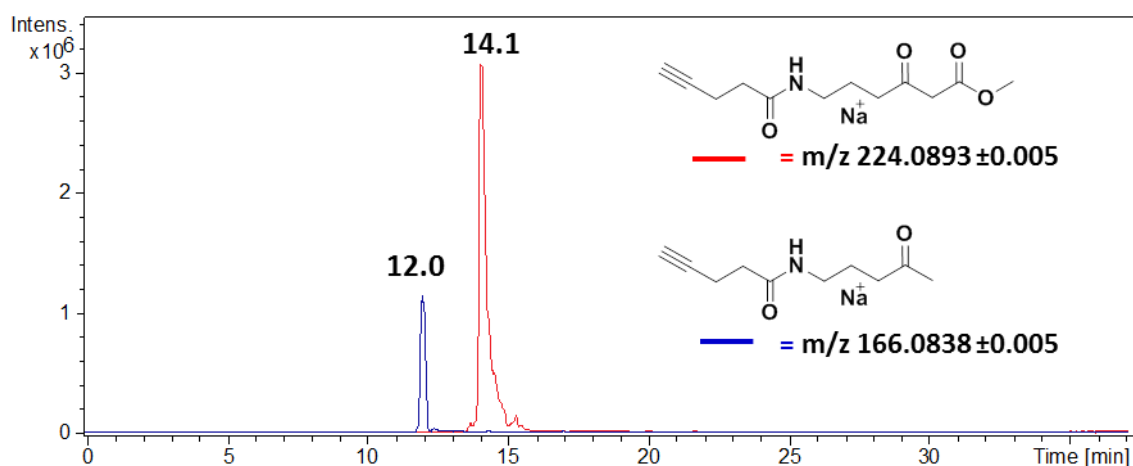


Figure S8. LC-MS/MS analyses of the organic extracts of *R. solanacearum* GMI1000 grown in the presence of probe 4: $[\text{M}+\text{Na}]^+$ extracted ion traces for the intact probe (red) and *N*-(4-oxopentyl)pent-4-ynamide (blue) resulting from *in vivo* hydrolysis and decarboxylation (Bruker MaXis Impact).

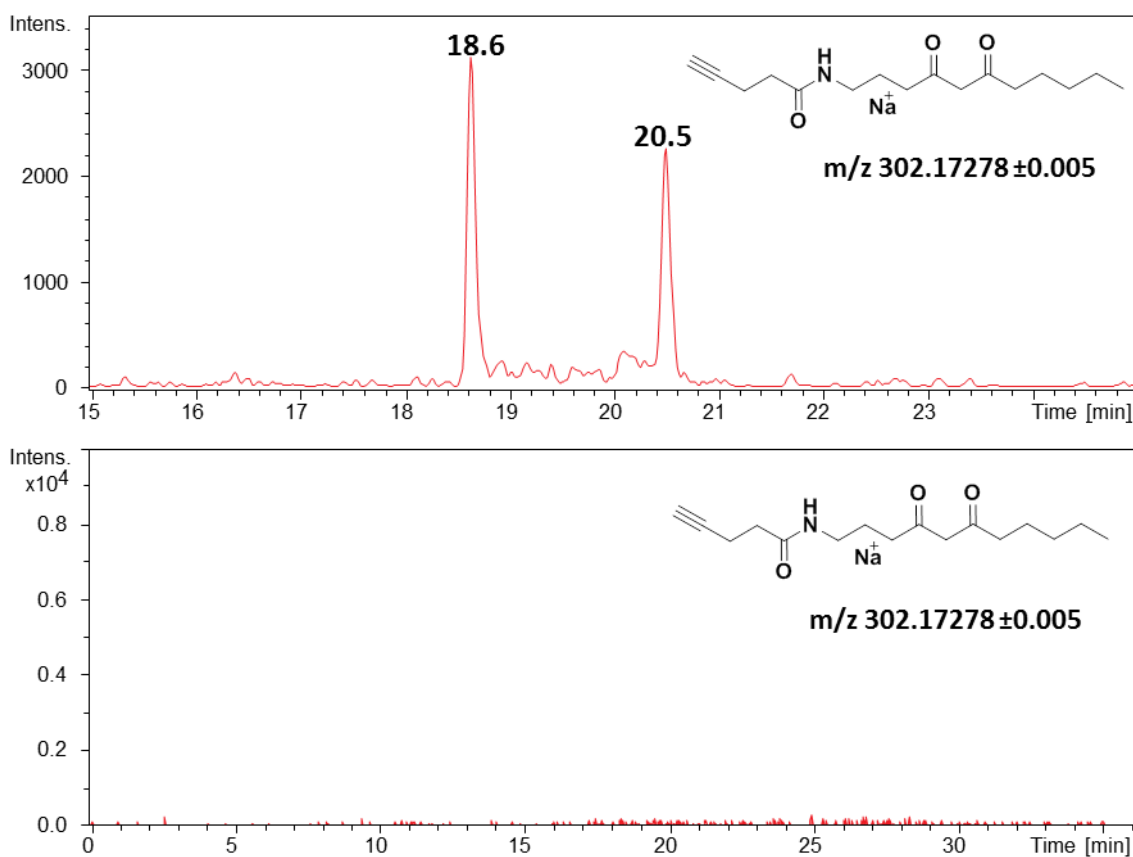


Figure S9. Top: $[M+Na]^+$ extracted ion traces for the putative diketides detected from *R. solanacearum* GMI1000 grown in the presence of probe 4; bottom: $[M+Na]^+$ extracted ion traces for the same species in a control sample of *R. solanacearum* GMI1000 grown in the absence of 4. The detection of two peaks for these species is currently under investigation (Bruker MaXis Impact).

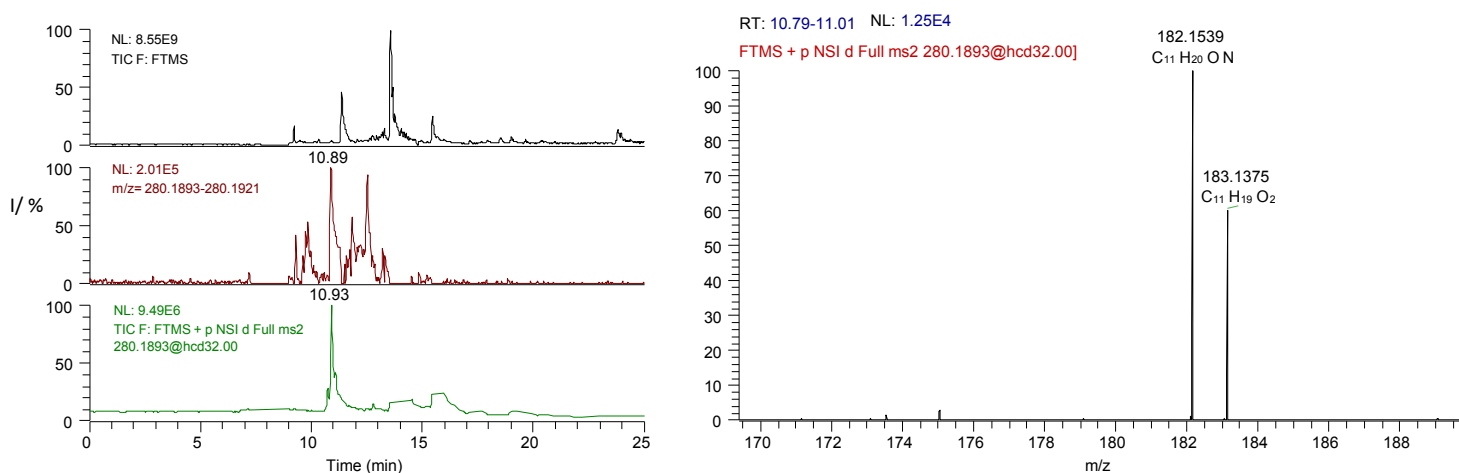
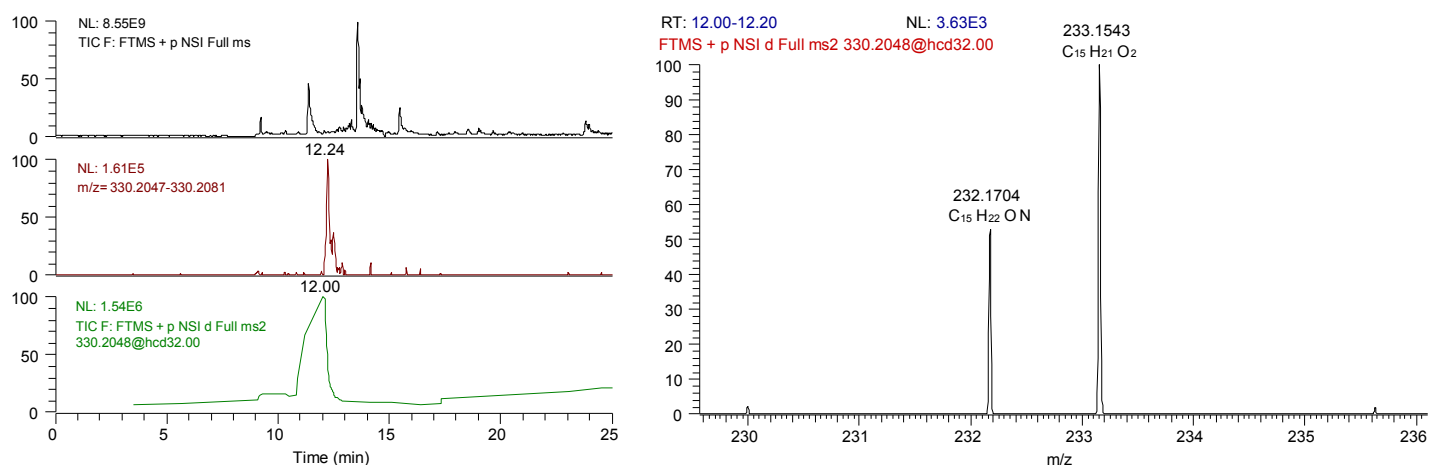
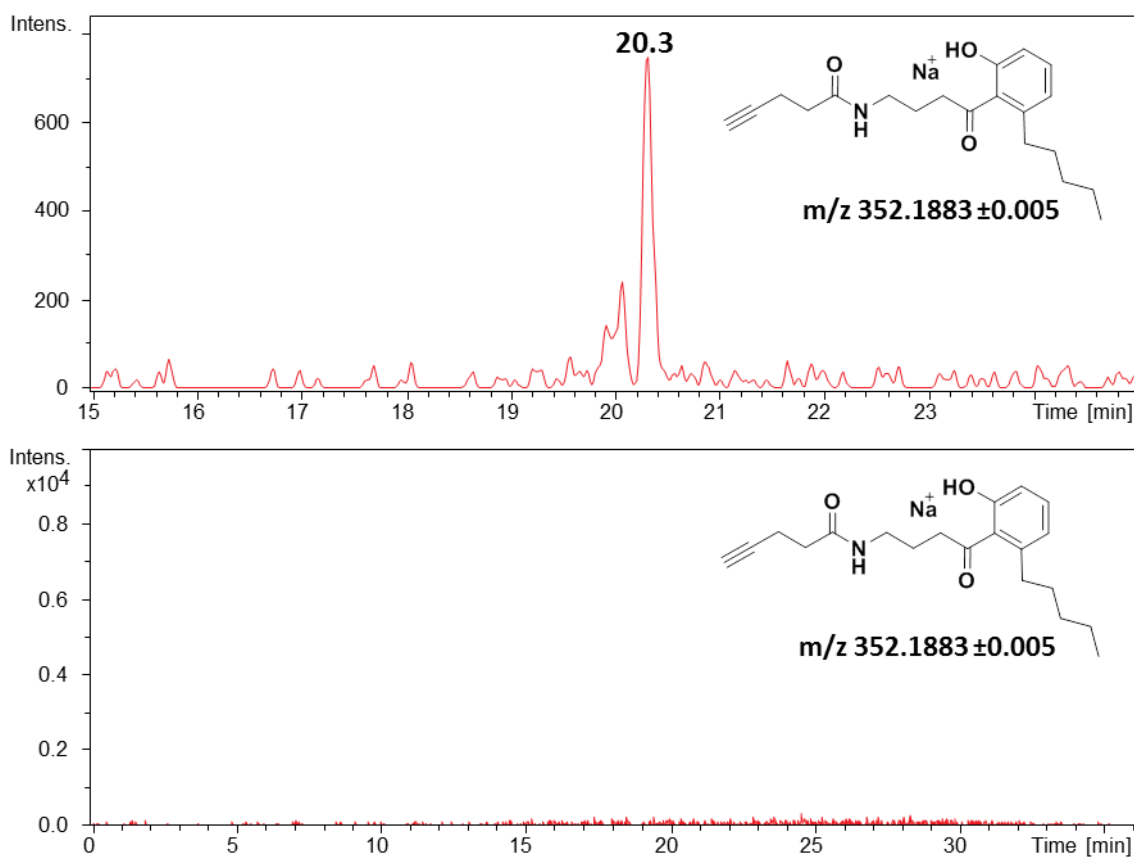


Figure S10. Left: TIC and $[M+H]^+$ extracted ion traces for the putative diketides detected from *R. solanacearum* GMI1000 grown in the presence of probe 4; right: putative diketide fragmentation (Thermo Orbitrap Fusion).



Intermediate capture by probe 5 (methyl 6-decanamido-3-oxohexanoate)⁸

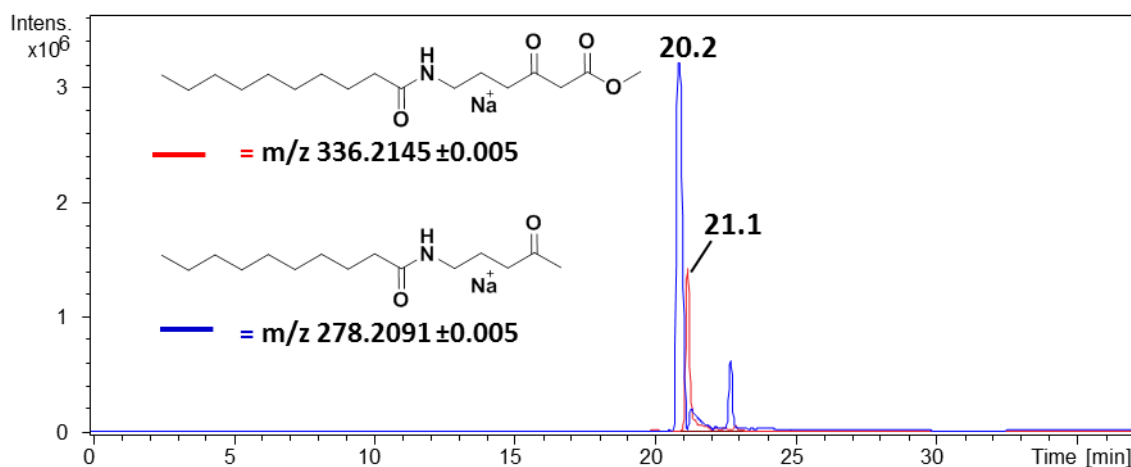


Figure S13. LC-HRMS analyses of the organic extracts of *R. solanacearum* GMI1000 grown in the presence of probe 5: [M+Na]⁺ extracted ion traces for the intact probe (red) and *N*-(4-oxopentyl)decanamide (blue) resulting from *in vivo* hydrolysis and decarboxylation (Bruker MaXis Impact).

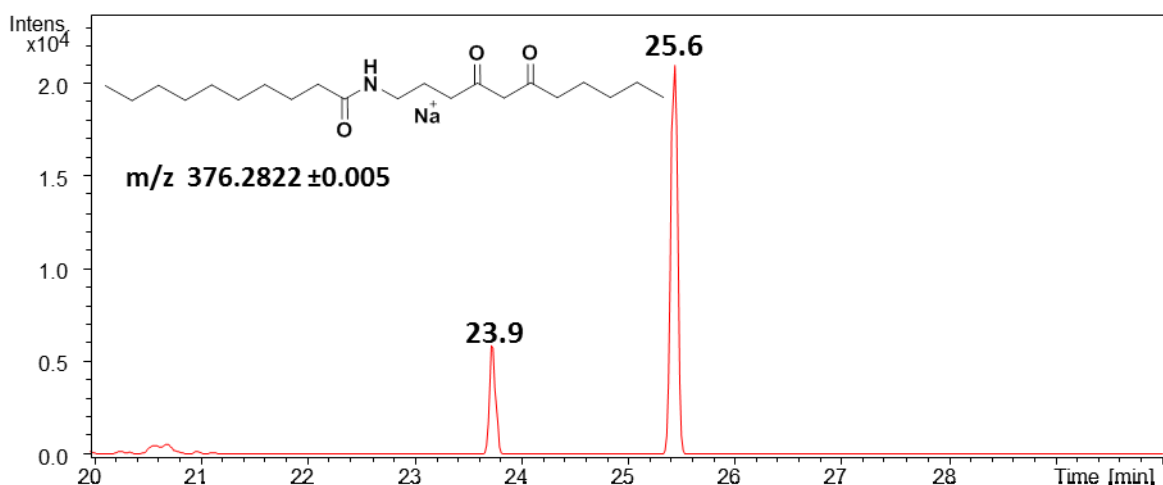


Figure S14. Top: [M+Na]⁺ extracted ion traces for the putative diketides detected from *R. solanacearum* GMI1000 grown in the presence of probe 5; bottom: [M+Na]⁺ extracted ion traces for the same species in a control sample of *R. solanacearum* GMI1000 grown in the absence of 5. The detection of two peaks for these species is currently under investigation (Bruker MaXis Impact).

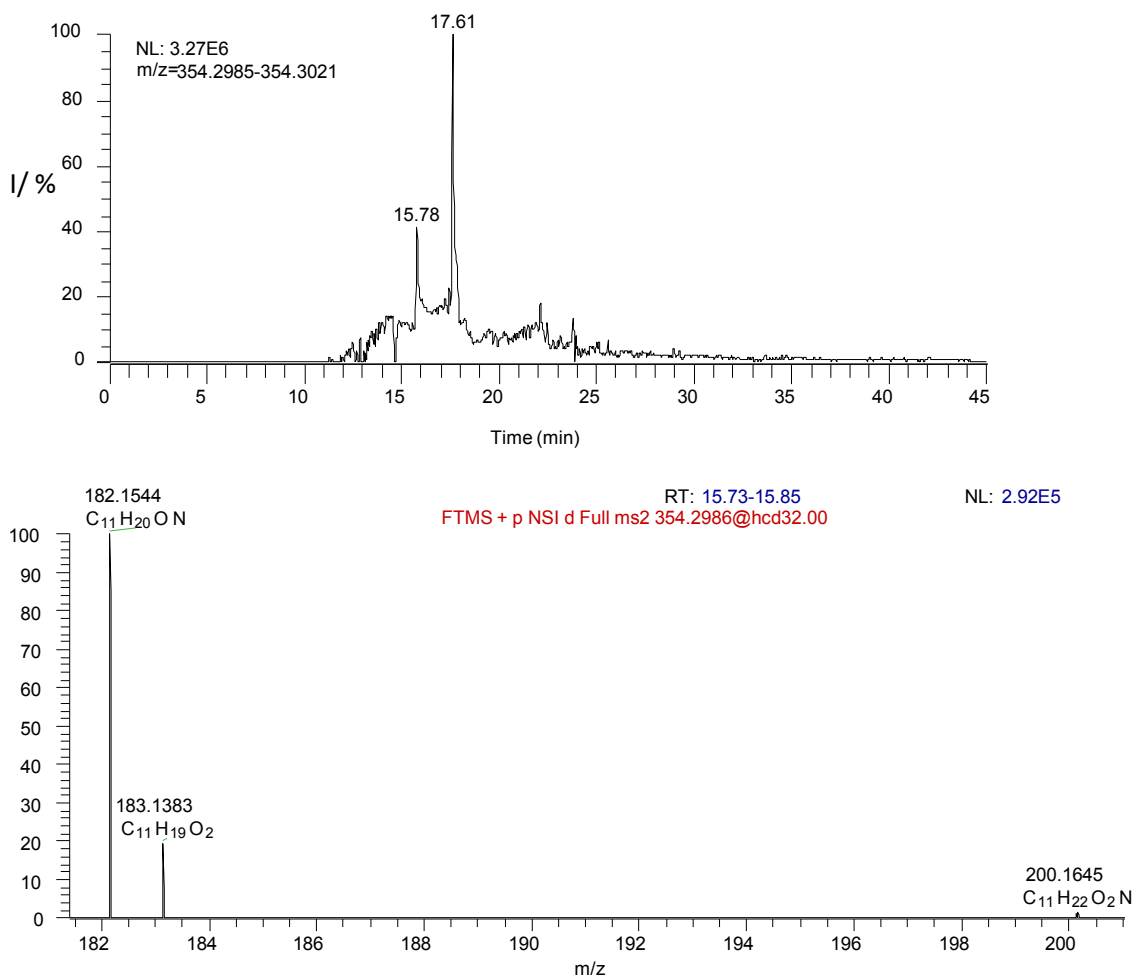


Figure S15. Top: $[M+H]^+$ extracted ion chromatogram for the putative diketide detected from *R. solanacearum* GMI1000 grown in the presence of probe 5; bottom: putative diketide fragmentation (Thermo Orbitrap Fusion).

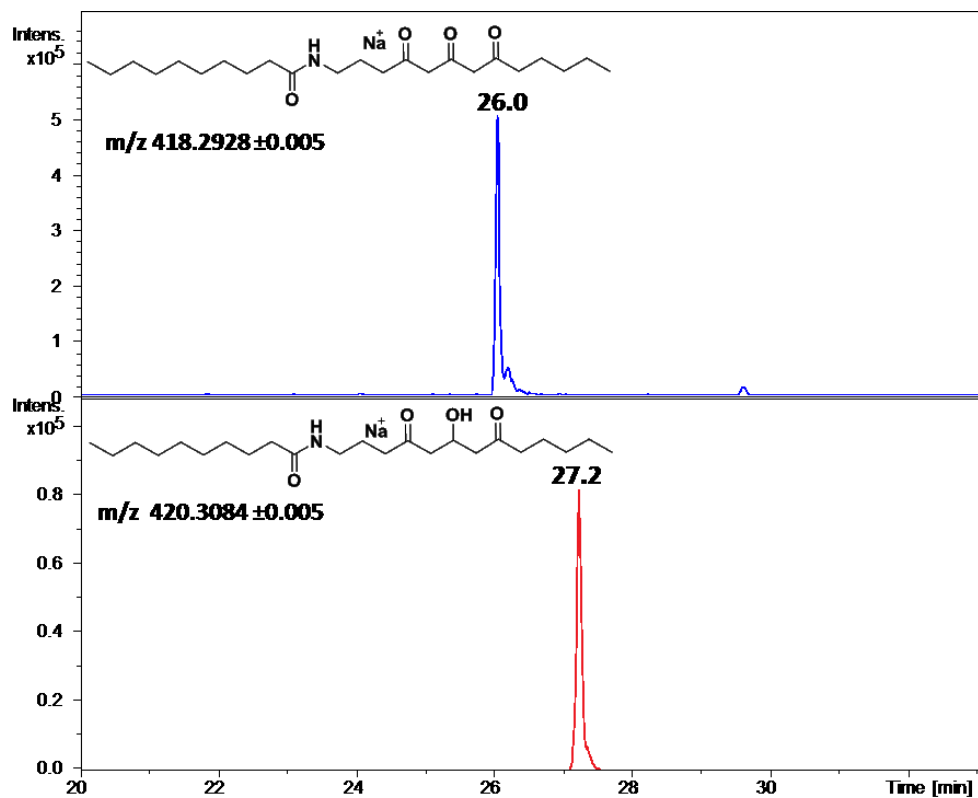


Figure S16. $[\text{M}+\text{Na}]^+$ extracted ion traces for the putative sodiated triketides detected from *R. solanacearum* GMI1000 grown in the presence of probe 5 (Bruker MaXis Impact).

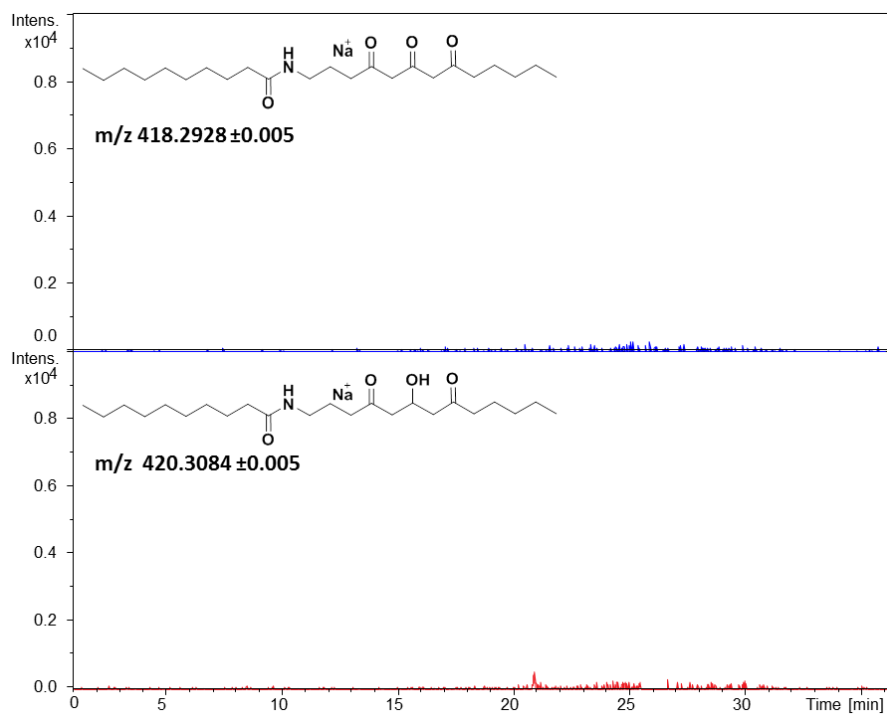


Figure S17. $[\text{M}+\text{Na}]^+$ extracted ion traces for the same species in a control sample of *R. solanacearum* GMI1000 grown in the absence of 5 (Bruker MaXis Impact).

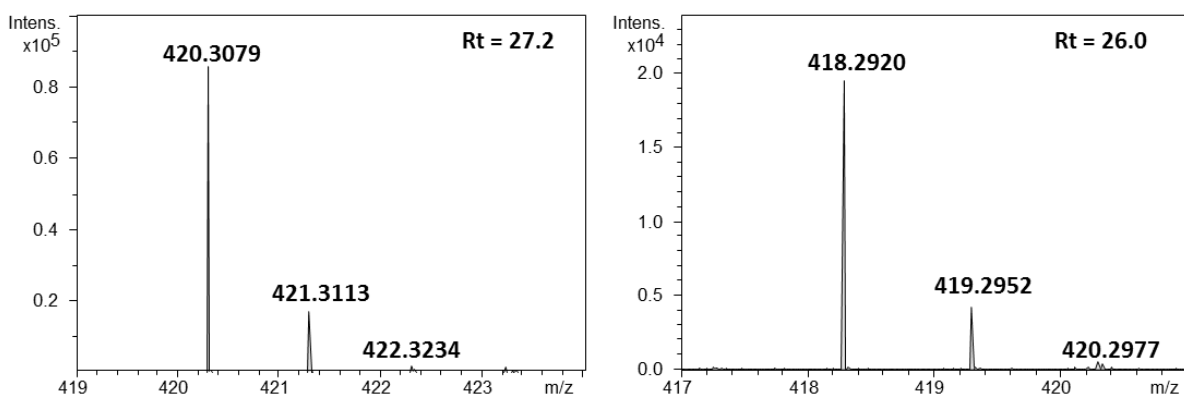


Figure S18. High resolution masses for sodiated triketides captured *via* probe 5 (Bruker MaXis Impact).

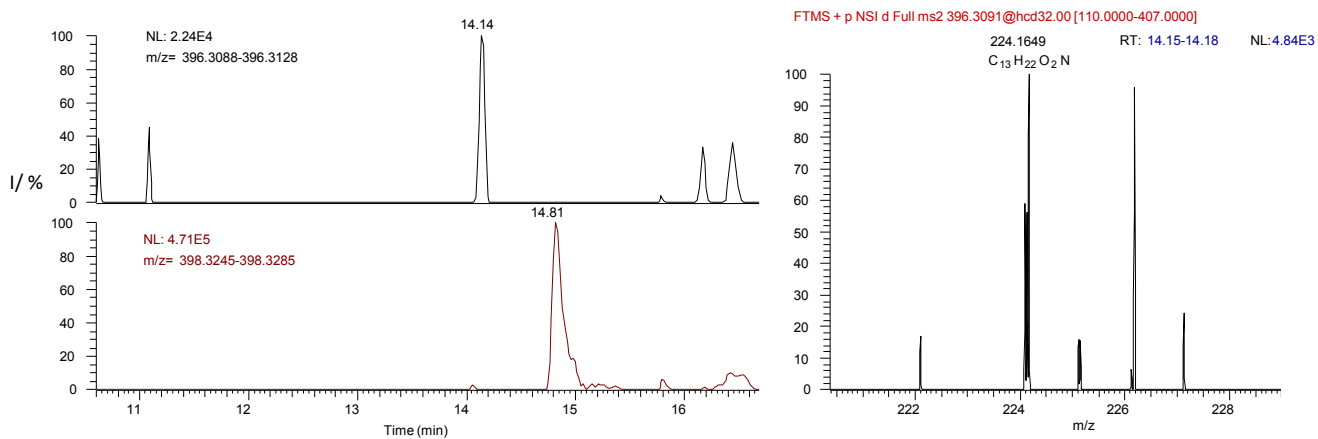


Figure S19. Left: $[M+H]^+$ extracted ion traces for the putative triketides detected from *R. solanacearum* GMI1000 grown in the presence of probe 5; right: fragmentation for the putative unreduced triketide (m/z 396, Thermo Orbitrap Fusion). The fragmentation for the putative reduced triketide is shown in Figure 2C of the main article.

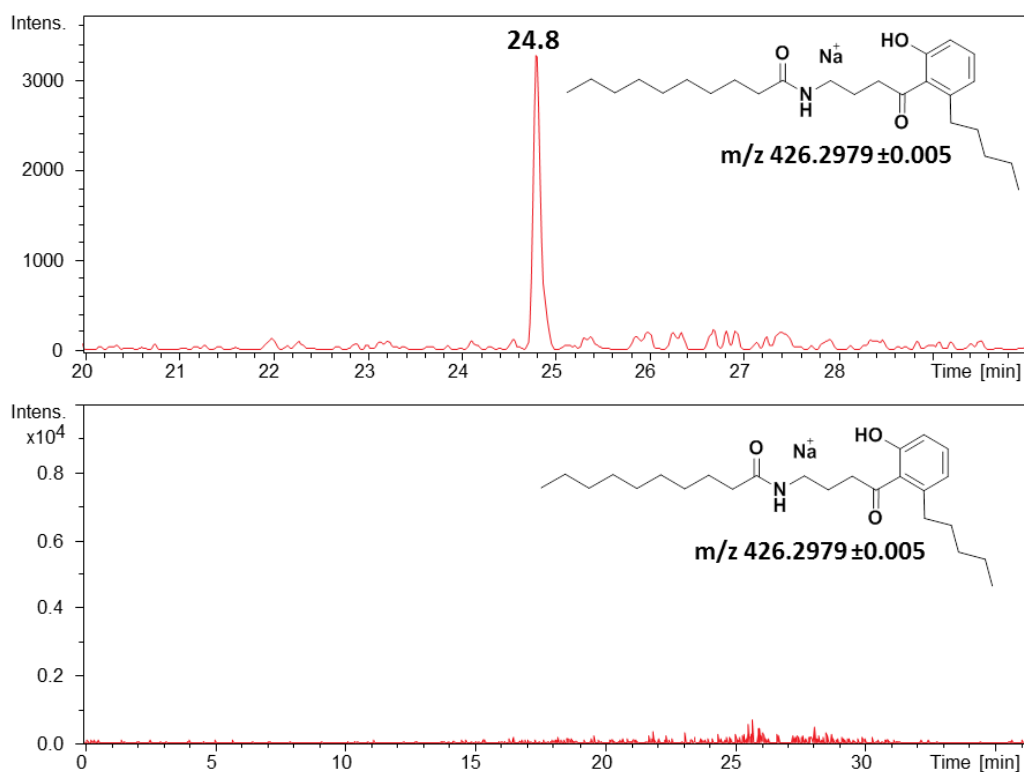


Figure S20. Top: $[M+Na]^+$ extracted ion traces for the putative aromatized tetraketide detected from *R. solanacearum* GMI1000 grown in the presence of probe 5; bottom: $[M+Na]^+$ extracted ion traces for the same species in a control sample of *R. solanacearum* GMI1000 grown in the absence of 5 (Bruker MaXis Impact).

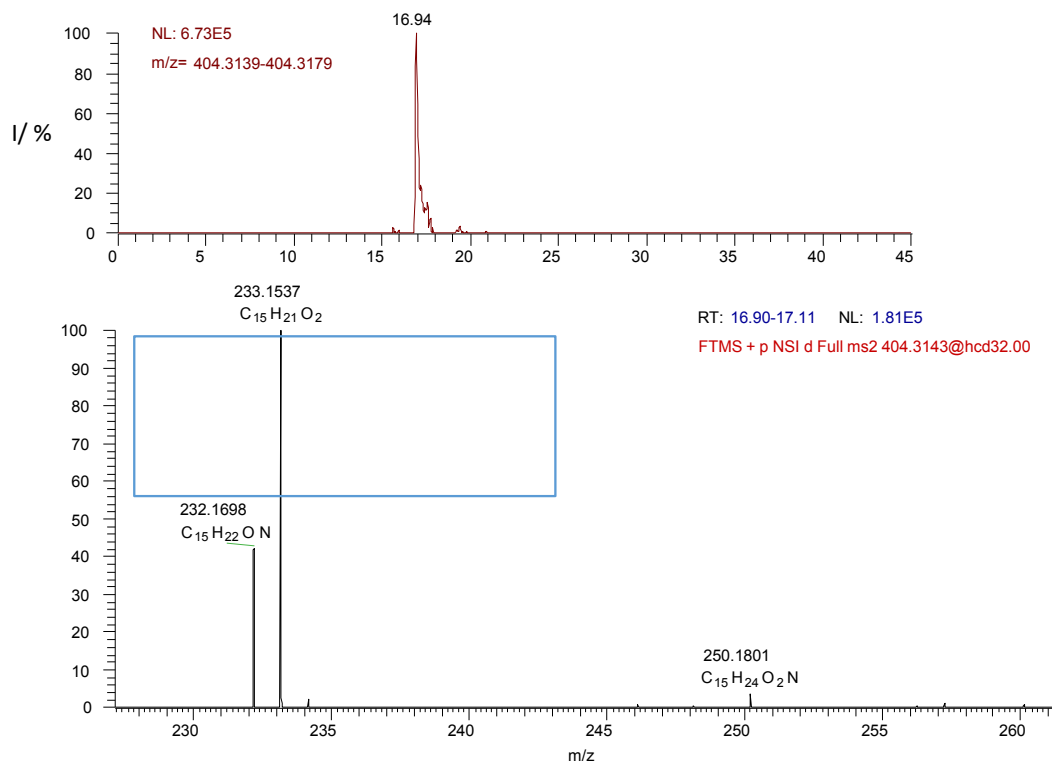


Figure S21. Top: $[M+H]^+$ extracted ion chromatogram for the putative tetraketide detected from *R. solanacearum* GMI1000 grown in the presence of probe 5; bottom: putative tetraketide fragmentation (Thermo Orbitrap Fusion).

References

- [1] C. A. Boucher, P. A. Barberis, A. P. Trigalet and D. A. Demery, *J. Gen. Microbiol.*, 1985, **131**, 2449.
- [2] M. F. Kreutzer, H. Kage, P. Gebhardt, B. Wackler, H. P. Saluz, D. Hoffmeister and M. Nett, *Appl. Environ. Microbiol.*, 2011, **77**, 6117.
- [3] M. Salanoubat, S. Genin, F. Artiguenave, J. Gouzy, S. Mangenot, M. Arlat, A. Billault, P. Brottier, J. C. Camus, L. Cattolico, M. Chandler, N. Choisne, C. Claudel-Renard, S. Cunnac, N. Demange, C. Gaspin, M. Lavie, A. Moisan, C. Robert, W. Saurin, T. Schiex, P. Siguier, P. Thébault, M. Whalen, P. Wincker, M. Levy, J. Weissenbach and C. A. Boucher, *Nature*, 2002, **415**, 497.
- [4] B. Gust, G. L. Challis, K. Fowler, T. Kieser and K. F. Chater, *Proc. Natl. Acad. Sci. U.S.A.*, 2003, **100**, 1541.
- [5] H. Kage, M. F. Kreutzer, B. Wackler, D. Hoffmeister and M. Nett, *Chem. Biol.*, 2013, **20**, 764.
- [6] J. L. Ried, and A. Collmer, *Gene*, 1987, **57**, 239.
- [7] (a) M. Tosin, L. Betancor, E. Stephens, W. M. Li, J. B. Spencer, P. F. Leadlay, *ChemBioChem*, 2010, **11**, 539; (b) M. Tosin, Y. Demydchuk, J. S. Parascandolo, C. B. Per, F. J. Leeper, P. F. Leadlay, *Chem. Commun.*, 2011, **47**, 3460.
- [8] E. Riva, I. Wilkening, S. Gazzola, W. M. A. Li, L. Smith, P. F. Leadlay, M. Tosin, *Angew. Chem. Int. Ed.*, 2014, **53**, 11944.